Cross sections of the *(n, p)* reaction on the ^{78}Se and ^{80}Se isotopes measured for 13.73 MeV to 14.77 MeV and estimated for 10 MeV to 20 MeV neutron energies

F. M. D. Attar,[1,*] S. D. Dhole,[2] and V. N. Bhoraskar[2,†]

[1]*Department of Physics, Ferguson College, Pune- 411004, India*

[2]*Department of Physics, S.P. Pune University, Pune- 411007, India*

The cross sections of ^{78}Se$(n, p)^{78}$As and ^{80}Se$(n, p)^{80}$As reactions were measured at five neutron energies over the range 13.73 MeV to 14.77 MeV using ^{56}Fe and ^{19}F as monitor elements, respectively. The cross sections were also theoretically estimated using EMPIRE-II and TALYS codes over 10 MeV to 20 MeV neutrons and matched with the experimental cross sections by making proper choice of the model parameters. The theoretical and experimental cross sections of ^{80}Se$(n, p)^{80}$As reaction are smaller as compared to the ^{78}Se$(n, p)^{78}$As reaction at each neutron energy. This difference is attributed to the competing ^{80}Se$(n, 2n)^{79}$Se and ^{80}Se$(n, \alpha)^{77}$Ge^{m} reactions, which effectively decrease the cross sections of ^{80}Se$(n, p)^{80}$As reaction as compared to that of the ^{78}Se$(n, p)^{78}$As reaction over the neutron energy range used in the present work. The cross sections of ^{78}Se$(n, p)^{78}$As and ^{80}Se$(n, p)^{80}$As reactions estimated by the EMPIRE-II code initially increase but later on decrease with neutron energy, respectively, above 16 MeV and 19 MeV, whereas those estimated by the TALYS code continuously increase with neutron energy. The present results indicate that the trends in the variation of cross section with neutron energy depend on the model used in the calculations. The cross sections of the ^{80}Se$(n, p)^{80}$As reaction at different neutron energies reported in the present work can be added as a new data in the nuclear data library.

I. INTRODUCTION

The neutron-induced reactions are important for a number of nuclear applications, and can be investigated by measuring the γ-ray activities of the reaction products. Some of the reactions exhibit specific characteristics of threshold energy, cross sections, emission of radiations, and decay half lives. Such reactions can also be used as monitors in fast neutron dosimeters as well as for elemental analysis. The data on the cross sections of the neutron-induced reactions are of importance for both the basic and applied research including nuclear technology, and most of these cross sections are given in the EXFOR database [1]. The cross sections for different nuclear reactions such as *(n, p)*, *(n, α)*, *(n, 2n)*, *(n, np)* have remained a field of interest for the past few decades [2,3]. For fusion reactors, accurate values of the cross sections for the *(n, p)* and *(n, α)* reactions are required for assessing and predicting the amount of hydrogen and helium gases trapped in the surrounding materials. The total cross sections for the *(n, p)* reactions are also of interest in the study of the primary and secondary damage induced in the materials as well as to assess formation of new isotopes in the vicinity of the reactor cores, neutron beam lines, and other high-flux neutron sources.

Selenium is a nonmetallic mineral and occurs naturally as a trace element in soils, rocks, water, and volcanic effluents. In nature, selenium is present as six stable isotopes; ^{74}Se, ^{76}Se, ^{77}Se, ^{78}Se, ^{80}Se, ^{82}Se, considering ^{82}Se as stable due to very long half life of 9.1×10^{19} years. In addition, there are 23 unstable radioisotopes of selenium so far identified.

The ^{79}Se radioisotope with half life 2.95×10^5 years, which decays by β emission is present normally in the spent nuclear fuels and waste nuclear material obtained after reprocessing of the nuclear fuel. Using proton-induced reactions, the ^{77}Se and ^{78}Se are converted to therapeutic radioisotope ^{77}Br, whereas ^{80}Se is used for the production of ^{80}Br^{m} required for other medical applications. In addition, selenium isotopes are also used as essential nutrient in some of the processed food items.

In general, arsenic has over 33 isotopes with mass number ranging from 60 to 92; out of these ^{75}As is a stable isotope. Arsenic is one of the most toxic elements found in nature and the lethal dose of arsenic oxide is close to 10 mg. The nuclear reactions such as Se*(n, p)*As produce arsenic isotopes and therefore the presence of selenium near a neutron source should be avoided. The reactions ^{78}Se$(n, p)^{78}$As and ^{80}Se$(n, p)^{80}$As are important because in a fast neutron environment the amount of arsenic produced from the existing selenium can be estimated. Moreover, the natural abundances of ^{78}Se and ^{80}Se are relatively high as compared to other stable isotopes of selenium.

In the present work, the activation cross sections for ^{78}Se$(n, p)^{78}$As and ^{80}Se$(n, p)^{80}$As reactions having negative Q values [4] have been measured at 13.73 MeV, 14.07 MeV, 14.42 MeV, 14.68 MeV, and 14.77 MeV neutron energies. The measured cross sections of these two reactions were compared with the cross sections estimated using the EMPIRE-II code [5] and TALYS code [6] over the neutron energy range 10 MeV to 20 MeV. Attempts were also made to use different values of the parameters, such as nuclear level density, nuclear reaction models, and nucleon potential, etc., to match the theoretically estimated cross sections with the cross sections measured in the present work as well as with those reported in the literature [1].

─────────

*Corresponding author: fmdattar@gmail.com

†Corresponding author: vnb@physics.unipune.ac.in

II. EXPERIMENT

A. Neutron irradiation

The neutron irradiation work was carried out at the 14 MeV neutron generator laboratory [7], Department of Physics, University of Pune, Pune, India. The 14 MeV neutrons were produced by bombarding deuterium ions of energy 175 keV on an 8 Curie tritium target. On the tritium target, the deuterium beam had a diameter ∼4 mm and current ∼100 μA.

For the study of ^{78}Se$(n, p)^{78}$As and ^{80}Se$(n, p)^{80}$As reactions, the samples were made from natural SeO$_2$(99.99%) powder. For the ^{78}Se$(n, p)^{78}$As reaction, Fe-56 isotope in the form of natural iron (99.99%) powder was used as monitor. Each sample was made by mixing a known weight of SeO$_2$ powder with a known weight of the iron powder, and packing it in a polyethylene bag. The total weight of the selenium powder and the iron powder was ∼1 g, measured with a microbalance at an accuracy of ±10 μg. The polyethylene bag was folded in such a way that the size of the powder sample was close to 10 mm ×10 mm. Fifteen such samples were made for studying ^{78}Se$(n, p)^{78}$As reaction with ^{56}Fe$(n, p)^{56}$Mn as monitor reaction. For the activation experiment, a semicircular plexiglass plate was horizontally fixed on a stainless steel rod such that the plane of the plate was parallel to the ground. On this plate angles from 0° to 120° were marked along the semicircle of 60 mm radius. The 0° position was along the line of the deuterium ions incident on the center of the tritium target. Out of these fifteen samples, five samples were mounted on the plexiglass plate such that one sample occupied one angular position respectively at 0°, 30°, 60°, 90°, and 120° on the marked positions. In this manner, each sample could be placed at a distance of 60 mm from the center of the tritium target. All the five samples were irradiated with neutrons simultaneously for a period of 5400 s. As per the energy distribution of the emitted neutrons, the samples mounted at 0°, 30°, 60°, 90°, and 120° angular position were irradiated respectively with 14.77 MeV, 14.68 MeV, 14.42 MeV, 14.07 MeV, and 13.73 MeV energy neutrons [8]. The decay data of the radioisotopes ^{78}As and ^{56}Mn produced through ^{78}Se$(n, p)^{78}$As and ^{56}Fe$(n, p)^{56}$Mn reactions respectively are given in Table I [9–11]. Following the same procedure, the experiment was repeated for three times and the cross sections of the reaction were obtained by taking average of three measurements, made at each angular position.

Following the same experimental procedure, the cross sections of ^{80}Se$(n, p)^{80}$As reaction at different neutron energies were measured using ^{19}F$(n, p)^{19}$O as monitor reaction. The half life of ^{80}As is 15.2 s whereas the half life of ^{19}O is 26.9 s.

For the study of this reaction, samples were made by mixing pure powder of CaF$_2$ (99.99%) with the powder of SeO$_2$. In this manner three sets of the samples, each set having five samples were made. In all these fifteen samples, the weight of each sample was ∼1 g. A pneumatic sample transfer system was used to transfer the sample from neutron irradiation head to HPGe detector and back to the neutron irradiation head. One sample at a time was irradiated with neutrons for a period of 60 s and then brought to the Γ-ray detector by the pneumatic transfer system. The decay data of the radioisotopes ^{80}As and ^{19}O produced through ^{80}Se$(n, p)^{80}$As and ^{19}F$(n, p)^{19}$O reactions respectively are given in Table I [9–11]. The induced γ-ray activity was measured for 60 s using the HPGe detector. After a cooling period of 60 s the sample was sent back for neutron irradiation. In this manner five cycles of neutron irradiation and γ-ray activity measurements were repeated for each sample kept at 0° angular position. After that another sample was kept at 30° position and five cycles of neutron irradiation and γ-ray activity measurements were repeated. Following the same experimental procedure, the activation experiments were repeated by irradiating samples at 60°, 90°, and 120°. The sample position was adjusted to bring it in front of the irradiation head of the neutron generator.

B. Measurement of γ-ray activity

The induced γ-ray activities of the irradiated samples were measured with the HPGe detector. The γ-ray detection efficiency of this detector was measured with a Canberra make Multi Γ Standard MGS-3 γ-ray source in a separate experiment. The energy calibration of the detector was also carried out using the MGS-3 γ source. After the end of the irradiation period, the sample was transferred to the counting room with the help of the pneumatic transfer system designed and developed in the laboratory. The induced γ-ray activity from ^{78}As (0.614 MeV) and ^{56}Mn (0.847 MeV) radioisotopes produced in the sample was measured for a period of 900 s. Initially the γ-ray activity of the sample irradiated at 0° position was measured. Later on the γ-ray activities of the samples irradiated at 30°, 60°, 90°, and 120° angular positions were measured in sequence.

For the sample irradiated at 0° position with reference to the neutron beam, the induced γ activity of (i) 0.614 MeV due to ^{78}As and (ii) 0.847 MeV due to ^{56}Mn were measured by HPGe detector kept in the measurement room. Following the same experimental procedure, the induced γ-ray activity of the remaining four samples irradiated at 30°, 60°, 90°, and 120° angular positions were measured sequentially. A total period of 20 s was kept between the end of counting the γ-ray

TABLE I. The decay data of the radioisotopes produced in neutron induced reactions [9–11].

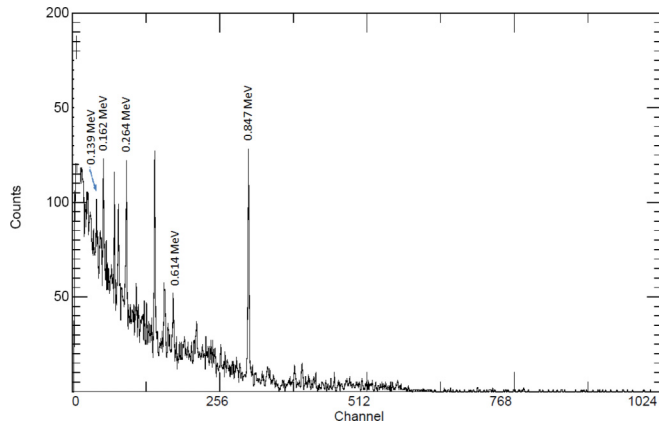| Nuclear Reaction	Abundance (%)	Half life	E_γ (MeV)	f_d (%)
^{78}Se$(n, p)^{78}$As	23.77 ± 0.28	90.7 ± 0.2 m	0.614	54 ± 0.6
^{80}Se$(n, p)^{80}$As	49.61 ± 0.41	15.2 ± 0.2 s	0.666	42 ± 0.5
^{56}Fe$(n, p)^{56}$Mn	91.75 ± 0.36	2.578 ± 0.0001 hr	0.847	99 ± 0.3
^{19}F$(n, p)^{19}$O	100	26.91 ± 0.08 s	0.197	96 ± 2.1
			1.357	50.4 ± 1.1

FIG. 1. (Color online) Γ-ray spectra of ^{78}As and ^{56}Mn radio nuclei produced by irradiating ^{78}Se and ^{56}Fe respectively with 13.73 MeV neutrons.

activity of the first sample and the start of the γ-ray activity counting of the second sample. Accordingly, the total cooling time for each sample was accounted while estimating the actual induced γ-ray activity.

In the case of ^{80}Se$(n, p)^{80}$As reaction, the pneumatic transfer system was also used to bring the neutron irradiated sample directly to the HPGe detector kept in the counting room. The induced γ-ray activity of (i) 0.666 MeV due to ^{80}As and (ii) 0.197 MeV due to ^{19}O were measured for a period of 60 s. A cooling period of 120 s was kept after the end of the γ-ray activity measurement period. Twenty activation cycles were repeated, each consisting of (i) neutron irradiation period of 60 s, (ii) γ-ray activity measurement period of 60 s, and (iii) cooling period of 60 s. The counting mode of MCA was switched off during the neutron irradiation period through a remote electronic system.

The radioisotope ^{16}N produced in ^{16}O$(n, p)^{16}$N reaction has half life 7.13 s and emits γ rays of 2.741 MeV (0.8%), 6.13 MeV (67%), and 7.11 MeV (4.9%) energies. These γ rays were discriminated by adjusting the upper level of the single channel analyzer. The radioisotope ^{77}Se^m produced in ^{78}Se$(n, 2n)^{77}$Se^m reaction has half life 17.36 s and emits γ
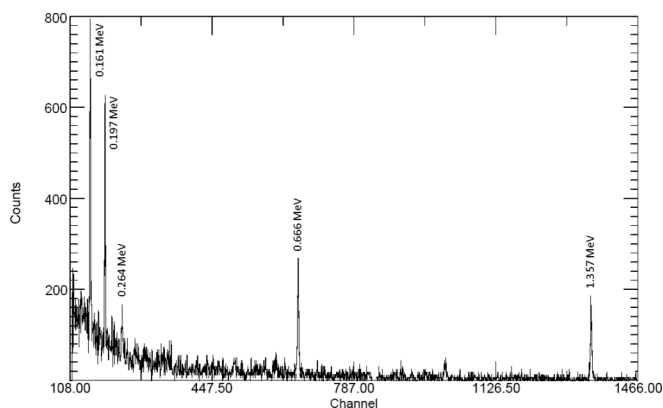

FIG. 2. Γ-ray spectra of ^{80}As and ^{19}O radio nuclei produced by irradiating ^{80}Se and ^{19}F respectively with 13.73 MeV neutrons.

ray of 0.161 MeV (53.2%). The photo peak of 0.161 MeV γ ray has appeared in the γ-ray spectra of ^{80}Se$(n, p)^{80}$As and ^{19}F$(n, p)^{19}$O reactions. In the γ-ray spectra of Figs. 1 and 2, the photo peak at 0.264 MeV is due to ^{75}Ge and ^{77}Ge^m radioisotopes produced respectively through ^{78}Se$(n, \alpha)^{75}$Ge, and ^{80}Se$(n, \alpha)^{77}$Ge^m reactions. It is observed in Fig. 1 and Fig. 2 that no radioisotope was produced from calcium present in the monitor sample.

III. DATA ANALYSIS

The nuclear data of the radioisotopes given in Table I was used for the present work. Figure 1 shows the γ-ray spectra of ^{78}As and ^{56}Mn radioisotopes, and Fig. 2 shows the γ-ray spectra of ^{80}As and ^{19}O radioisotopes produced respectively through the nuclear reactions induced by neutrons. The activation cross sections for the ^{78}Se$(n, p)^{78}$As and ^{80}Se$(n, p)^{80}$As reactions were obtained at 13.73 MeV, 14.07 MeV, 14.42 MeV, 14.68 MeV, and 14.77 MeV neutron energies using the following activation expression (1),

$$\sigma = \sigma_M \frac{A \varepsilon_M f_{dM} \lambda}{A_M \varepsilon f_d \lambda_M} \frac{N_M}{N} \frac{(1 - e^{-\lambda_M t_1})}{(1 - e^{-\lambda t_1})} \frac{e^{-\lambda_M t_2}}{e^{-\lambda t_2}} \frac{(1 - e^{-\lambda_M t_3})}{(1 - e^{-\lambda t_3})},$$
(1)

where σ is the reaction cross section, A is the number of counts under the photo peak, f_d is the photon disintegration probability, ε is the detector efficiency, σ_M is the cross section for monitor reaction, λ is the decay constant, N is the number of atoms of the isotope of the element, t_1 is the irradiation time, t_2 is the cooling time, and t_3 is the period for which the γ activity is measured. The quantity with the subscript M stands for the monitor reaction.

By considering the uncertainties involved in the measurement of each parameter, the error analysis was carried out using the quadrature method [12]. The flux of low-energy neutrons ($E_n < 10$ MeV) produced in the D-T reaction is about two orders of magnitude lower than that at 14 MeV energy [13], and therefore not considered in the estimation of the cross sections of both the reactions. Similarly, the effects of the multiple scattering of neutrons and inhomogeneities in the sample were neglected as the errors contributed by these processes are negligibly small. The estimated errors in the different parameters are as follows; (i) detector efficiency ($\sim$1.5%); (ii) self absorption of γ rays ($<$14%) [14]; (iii) neutron energy

TABLE II. Measured cross sections of the ^{78}Se$(n, p)^{78}$As and ^{80}Se$(n, p)^{80}$As nuclear reactions over 13.73 MeV to 14.77 MeV neutron energies.

Neutron energy (MeV)	Measured cross section (mb)	
	^{78}Se$(n, p)^{78}$As	^{80}Se$(n, p)^{80}$As
13.73	15.6 ± 1.5	4.8 ± 0.63
14.07	17 ± 1.6	7.1 ± 0.95
14.42	18.6 ± 1.6	8.6 ± 1.1
14.68	20.4 ± 1.7	9.6 ± 1.4
14.77	22 ± 1.7	11 ± 1.6

distribution ($<1\%$); (iv) absolute γ-ray intensity ($<2.2\%$); (v) reference cross section of the reaction ^{56}Fe(n, p)^{56}Mn (2–3.7%) [15]; and (vi) reference cross section of ^{19}F(n, p)^{19}O reaction ($<5.28\%$) [16].

The cross sections of the nuclear reactions ^{78}Se(n, p)^{78}As and ^{80}Se(n, p)^{80}As measured at 13.73 MeV, 14.07 MeV, 14.42 MeV, 14.68 MeV, and 14.77 MeV neutron energies are given in Table II.

IV. NUCLEAR MODEL CALCULATIONS

The theoretical cross sections for ^{78}Se(n, p)^{78}As and ^{80}Se(n, p)^{80}As reactions were estimated using statistical nuclear models EMPIRE-II code [5] and TALYS code [6] over 10 MeV to 20 MeV neutron energies. In these codes, a number of options are available mainly for nuclear level density, nuclear reaction models, etc. Initially the choice of the parameters was made to obtain good matching between the theoretical cross sections with those measured in the present work over 13.73 MeV to 14.77 MeV neutron energies by considering the possible reaction channels depending on the compound nucleus energy. Using these options the theoretical cross sections of these reactions were estimated over 10 MeV to 20 MeV neutron energies by EMPIRE-II and TALYS codes.

A. EMPIRE-II code

The cross sections for ^{78}Se(n, p)^{78}As and ^{80}Se(n, p)^{80}As reactions were estimated using the exciton model DEGAS [17] and also using multistep compound [18] and multistep direct models [19].

The level density options, namely (i) EMPIRE-specific [20]; (ii) Fermi gas [21]; (iii) Gilbert-Cameron [22]; and (iv) Hartree-Fock-BCS (HF-BCS) approach [23] were used for estimating the cross sections over the neutron energy range 13.73 MeV to 14.77 MeV of the measurement. Moreover, in these calculations, for each level density, the optical potentials for neutrons and protons given by Koning [24] and Bechetti [25] were used. A comparison between the estimated cross sections with those measured in the present work provided important information about the best option of the parameters. Furthermore, using the best options of the parameters and their combinations, the cross sections for ^{78}Se(n, p)^{78}As and ^{80}Se(n, p)^{80}As reactions were estimated over 10 MeV to 20 MeV neutron energies by EMPIRE-II code.

B. TALYS code

The TALYS code [6] was also used for estimating the cross sections of ^{78}Se(n, p)^{78}As and ^{80}Se(n, p)^{80}As reactions over neutron energy range 10 MeV to 20 MeV. The main approach provided in the TALYS code was followed using different options of level densities namely ldmodel 1 [20,21], ldmodel 2 [21,26,27], and ldmodel 3 [28]. The ldmodel 1 uses Fermi gas level density with effective level density for the ground state, and the collective effects on the barrier determined relative to the ground state. The ldmodel 2 uses Fermi gas level density with explicit rotational and vibrational enhancement on ground state and fission barrier, whereas the

ldmodel 3 uses microscopic level densities obtained from Goriely's table [28]. These calculations were performed using the optical model parameters of neutrons, protons given by Koning [24], exciton model [29–31] preeqmode 1, and also using multistep compound and multistep direct model preeqmode 4 [32,33]. Initially, the calculations were carried out over 13.73 MeV to 14.77 MeV neutron energies using all the three level densities to find out the best option of the parameters. The parameters that produced theoretical cross sections close to those measured over 13.73 MeV to 14.77 MeV neutron energies were used for estimating the cross sections for ^{78}Se(n, p)^{78}As and ^{80}Se(n, p)^{80}As reactions over 10 MeV to 20 MeV neutron energies.

V. RESULTS AND DISCUSSION

The recorded γ-ray spectra of (i) ^{78}As and ^{56}Mn radioisotopes produced respectively in ^{78}Se(n, p)^{78}As and ^{56}Fe(n, p)^{56}Mn reactions are shown in Fig. 1, and that of (ii) ^{80}As and ^{19}O radioisotopes produced respectively in ^{80}Se(n, p)^{80}As and ^{19}F(n, p)^{19}O reactions are shown in Fig. 2. The γ-ray spectra shown in Figs. 1 and 2 are background subtracted and therefore the area under each photo peak is proportional to the respective γ-ray activity induced in the sample. The experimental cross sections for ^{78}Se(n, p)^{78}As and ^{80}Se(n, p)^{80}As reactions were obtained at 13.73 MeV, 14.07 MeV, 14.42 MeV, 14.68 MeV, and 14.77 MeV neutron energies by substituting values of all the experimental parameters and constants in the activation expression (1) and the values of the cross sections are given in Table II. It is evident from Table II that over neutron energies 13.73 MeV to 14.77 MeV, the cross sections of (i) ^{78}Se(n, p)^{78}As reaction varies from 15.6 mb to 22 mb and (ii) that of ^{80}Se(n, p)^{80}As reaction varies from 4.8 mb to 11 mb.

Considering the available options of the level densities and nucleon potentials in EMPIRE-II code, the cross sections for ^{78}Se(n, p)^{78}As reaction over 13.73 MeV to 14.77 MeV neutron energies (i) estimated using exciton model DEGAS are given in Table III and (ii) those estimated using multistep compound and multistep direct model are given in Table IV. Similarly, the cross sections of ^{78}Se(n, p)^{78}As reaction over 13.73 MeV to 14.77 MeV neutron energies estimated by TALYS code using ldmodel 1, ldmodel 2, and ldmodel 3 level densities and considering exciton model preeqmode 1 are given in Table V.

On comparing the theoretically estimated cross sections given in Tables III and IV with the respective measured cross sections given in Table II, it is observed that the cross sections estimated by EMPIRE-II code (i) using EMPIRE-specific level density and optical potentials of Bechetti as well as (ii) using Hartree-Fock-BCS level density and Koning potentials are close to the corresponding cross sections measured in the present work over 13.73 MeV to 14.77 MeV neutron energies. Similarly, the cross sections estimated by TALYS code using Fermi gas level density (ldmodel 1) and considering exciton model preeqmode 1 are close to the corresponding cross sections over 13.73 MeV to 14.77 MeV neutron energies measured in the present work.

TABLE III. Cross sections for ^{78}Se$(n, p)^{78}$As reaction estimated over 13.73 MeV to 14.77 MeV neutron energies using different level density and nucleon potential options of EMPIRE-II code and considering exciton model DEGAS.

Neutron energy (MeV)	Theoretical cross section (mb)							
	EMPIRE specific		Fermi gas		Gilbert Cameron		Hartree-Fock-BCS	
	KG[a]	FDB[b]	KG	FDB	KG	FDB	KG	FDB
13.73	12.11	13.67	9	9.99	11.6	12.81	19.6	22.32
14.07	13.54	15.28	10	11.1	12.5	13.81	21.5	24.45
14.42	14.94	16.85	10.9	12.12	13.3	14.74	23.4	26.52
14.68	15.46	17.40	11.2	12.46	13.4	14.77	24.1	27.19
14.77	15.82	17.79	11.5	12.74	13.6	14.99	24.5	27.66

[a]Koning Global potential.
[b]FDB-Bechetti potential.

Table VI gives a summary of the cross sections for ^{78}Se$(n, p)^{78}$As reaction (i) measured in the present work and (ii) estimated by EMPIRE-II and TALYS codes using the best options of the model parameters. Using these best options of the parameters given in Table VI, the cross sections of ^{78}Se$(n, p)^{78}$As reaction were estimated using EMPIRE-II and TALYS codes over 10 MeV to 20 MeV neutron energies and the results are given in Fig. 3. In addition, the cross sections reported in literature [34–38] and the cross sections measured in the present work are plotted in Fig. 3.

The plots in Fig. 3 show that, the theoretical cross sections obtained using EMPIRE-II and TALYS codes are close to the cross sections measured in the present work as well as those reported in literature. The results given in Fig. 3 revealed that below 13.4 MeV neutron energy, the cross sections reported by Birn [36] and Hoang [38] are higher as compared to those obtained using EMPIRE-II and TALYS codes. Moreover, above 15 MeV neutron energy, the cross sections measured by Hoang [38] are close to the cross sections estimated by EMPIRE-II code using both exciton model DEGAS and multistep compound and multistep direct model as compared to those estimated using TALYS code. In addition, it is also observed in Fig. 3 that the cross sections estimated using TALYS code increase with the increase in the neutron energy from 10 MeV to 20 MeV. These results of TALYS code are in general agreement with the JENDL 3.3 [4] and ENDF/B-VII.1 [39] evaluated cross sections.

However, the cross sections for this reaction estimated using EMPIRE-II code decrease with the increase in the neutron energy above 16 MeV and therefore do not agree with the JENDL 3.3 and ENDF/B-VII.1 cross sections. Furthermore, for ^{78}Se$(n, p)^{78}$As reaction the cross sections were also estimated by TALYS code using multistep compound and multistep direct model. However, these estimated cross sections were much higher as compared to the cross sections measured and also estimated using EMPIRE-II code in the present work as well as those reported in literature. These cross sections estimated by TALYS code using multistep compound and multistep direct model are therefore not given and discussed in this paper.

It is observed in literature [40] that the cross section of ^{80}Se$(n, p)^{80}$As reaction is reported only at 14.7 MeV neutron energy, and therefore in the present work the cross sections for this reaction were measured over 13.73 MeV to 14.77 MeV neutron energies. Moreover, the cross sections for this reaction at 13.73 MeV, 14.07 MeV, 14.42 MeV, 14.68 MeV, and 14.77 MeV neutron energies (i) estimated by EMPIRE-II code using the available options of level density, nucleon potential and considering exciton model DEGAS are given inTable VII and (ii) those estimated by TALYS code considering exciton model preeqmode 1 with ldmodel 1, ldmodel 2 and ldmodel 3 level densities are given in Table VIII.

Table IX gives a summary of the cross sections for ^{80}Se$(n, p)^{80}$As reaction over 13.73 MeV to 14.77 MeV neutron

TABLE IV. Cross sections for ^{78}Se$(n, p)^{78}$As reaction estimated over 13.73 MeV to 14.77 MeV neutron energies using different level density and nucleon potential options of EMPIRE-II code and considering multistep compound and multistep direct model.

Neutron energy (MeV)	Theoretical cross section (mb)							
	EMPIRE specific		Fermi gas		Gilbert Cameron		Hartree-Fock-BCS	
	KG[a]	FDB[b]	KG	FDB	KG	FDB	KG	FDB
13.73	8.26	10.05	4.88	5.98	7.68	9.09	16.39	19.59
14.07	9.17	11.13	5.3	6.5	8.01	9.5	17.87	21.27
14.42	10.11	12.25	5.74	7.04	8.35	9.93	19.28	22.89
14.68	10.59	12.78	5.96	7.29	8.31	9.87	20.00	23.64
14.77	10.74	12.96	6.02	7.36	8.3	9.86	20.21	23.84

[a]Koning Global potential.
[b]FDB-Bechetti potential.

TABLE V. Cross sections for ^{78}Se$(n, p)^{78}$As reaction estimated over 13.73 MeV to 14.77 MeV neutron energies using different level density options of TALYS code and considering exciton model preeqmode 1.

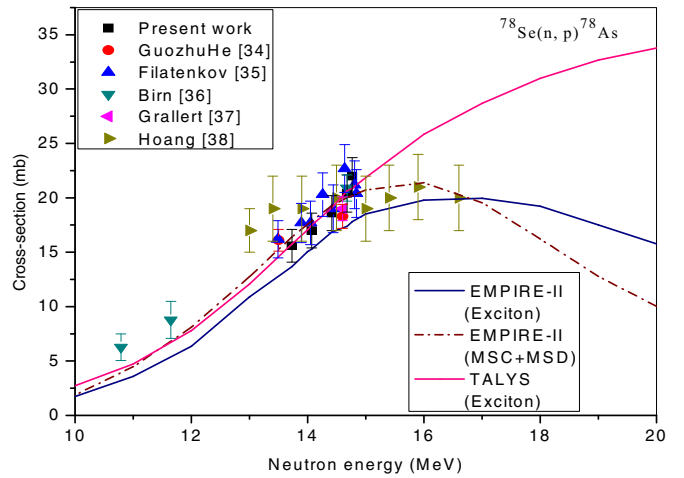| Neutron energy (MeV)	Theoretical cross section (mb)		
	ldmodel 1	ldmodel 2	ldmodel 3
13.73	15.75	19.11	22.54
14.07	17.48	20.95	24.96
14.42	19.09	22.69	27.26
14.68	20.64	24.38	29.27
14.77	20.87	24.57	29.62

FIG. 3. (Color online) Cross sections for ^{78}Se$(n, p)^{78}$As reaction at different neutron energies (i) measured in the present work and (ii) estimated over 10 MeV to 20 MeV neutron energies using EMPIRE-II and TALYS codes in the present work. A few literature cross sections are plotted for comparison.

energies (i) measured in the present work and (ii) estimated by EMPIRE-II and TALYS codes using the best options of the model parameters. Using the best options of the parameters given in Table IX, the cross sections of ^{80}Se$(n, p)^{80}$As reaction over 10 MeV to 20 MeV neutron energies were estimated by EMPIRE-II and TALYS codes and the results are plotted in Fig. 4. In addition, the literature cross section [40] and the cross sections measured in the present work are also plotted in Fig. 4.

It is observed in Table VII that the cross sections of ^{80}Se$(n, p)^{80}$As reaction estimated by exciton model DEGAS with EMPIRE-specific level density and nucleon potentials of Bechetti are close to the experimental cross sections as compared to those obtained by using other options of level densities and nucleon potentials. Similarly it is observed in Table VIII that the cross sections estimated by TALYS code using exciton model and ldmodel 3 level density are close to the cross sections measured in the present work as compared to those obtained using ldmodel 1 level density. As observed in Fig. 4, the cross section of ^{80}Se$(n, p)^{80}$As reaction reported by Minetti [40] at 14.7 MeV neutron energy is higher as compared to the cross section measured around 14.7 MeV as well as with the cross sections estimated using both the codes in the present work.

However, the cross sections for ^{80}Se$(n, p)^{80}$As reaction estimated using the multistep compound and multistep direct model in EMPIRE-II code are found to be lower and does not match with the cross sections measured in the present work and therefore these results are not given and discussed in

this paper. Similarly, the cross sections estimated by TALYS code using the multistep compound and multistep direct model were much higher as compared to the cross sections measured in the present work and also with only one cross section in literature. Therefore the cross sections estimated by TALYS code using the multistep compound and multistep direct model not considered worth reporting in this paper.

A comparison of the cross sections given in Table VI and Table IX show that the theoretically estimated and the experimental cross sections for ^{78}Se$(n, p)^{78}$As reaction are higher as compared to that of ^{80}Se$(n, p)^{80}$As reaction at all the neutron energies reported in the present work.

The ^{80}Se$(n, \alpha)^{77}$Ge reaction leads to the formation of the germanium metastable state ^{77}Ge^m having a lifetime of 52.9 s. By emitting a γ-ray of energy 0.159 MeV, the ^{77}Ge^m state decays to the ground state ^{77}Ge, which is radioactive with life time of 11.3 hours. Subsequently, by emitting a β particle ^{77}Ge decays to ^{77}As having lifetime of 38.83 hours.

The reaction ^{80}Se$(n, \alpha)^{77}$Ge^m competes with ^{80}Se$(n, p)^{80}$As reaction at all the neutron energies above the threshold, and therefore indirectly reduces the cross section

TABLE VI. Cross sections for ^{78}Se$(n, p)^{78}$As reaction (i) measured in the present work and (ii) theoretically estimated using EMPIRE-II and TALYS codes over 13.73 MeV to 14.77 MeV neutron energies using the best close options.

Neutron energy (MeV)	Theoretical cross section (mb)			Measured cross section (mb)
	EMPIRE-II		TALYS	
	Exciton model EMPIRE specific & Bechetti	MSC+MSD HFBCS & Koning	Exciton model ldmodel 1	
13.73	13.67	16.39	15.75	15.6 ± 1.5
14.07	15.28	17.87	17.48	17 ± 1.6
14.42	16.85	19.28	19.09	18.6 ± 1.6
14.68	17.4	20.00	20.64	20.4 ± 1.7
14.77	17.79	20.21	20.87	22 ± 1.7

TABLE VII. Cross sections for ^{80}Se$(n, p)^{80}$As reaction estimated over 13.73 MeV to 14.77 MeV neutron energies using different level density and nucleon potential options of EMPIRE-II code and considering exciton model DEGAS.

Neutron energy (MeV)	Theoretical cross section (mb)							
	EMPIRE specific		Fermi gas		Gilbert Cameron		Hartree-Fock-BCS	
	KG[a]	FDB[b]	KG	FDB	KG	FDB	KG	FDB
13.73	5.07	5.97	3.81	4.37	3.12	3.49	3.40	3.89
14.07	6.08	7.13	4.55	5.20	3.68	4.11	4.08	4.64
14.42	7.4	8.64	5.56	6.33	4.51	5.02	5.02	5.68
14.68	8.22	9.57	6.15	6.99	4.96	5.51	5.55	6.27
14.77	8.06	9.41	5.99	6.83	4.74	5.28	5.37	6.07

[a]Koning Global potential.
[b]FDB-Bechetti potential.

of ^{80}Se$(n, p)^{80}$As reaction. In addition, the theoretical cross sections of the ^{80}Se$(n, 2n)^{79}$Se reaction are higher than the corresponding cross section of ^{78}Se$(n, 2n)^{77}$Se reaction almost at all the neutron energies reported in the present work. This may be attributed to the two neutrons, which are excess in the ^{80}Se target nuclei as compared to ^{78}Se nuclei. In case of ^{80}Se the neutron emission probability through $(n, 2n)$ reaction is therefore higher as compared to that of ^{78}Se nuclei.

In addition, the radio nuclei ^{77}Ge and ^{75}Ge are also produced through ^{80}Se$(n, \alpha)^{77}$Ge and ^{78}Se$(n, \alpha)^{75}$Ge reactions respectively. The ^{77}Ge has a half life of about 11.3 hr and emits 0.264 MeV γ rays with 54% disintegration probability. Similarly the ^{75}Ge has a half life of 82.78 m and emits 0.264 MeV γ rays with 11% disintegration probability. In the recorded γ-ray spectrum shown in Fig. 2, the photo peak of 0.264 MeV energy had therefore contributions from both ^{77}Ge and ^{75}Ge radioisotopes. Even though the cross section for the ^{80}Se$(n, p)^{80}$As reaction is nearly equal to that of the ^{80}Se$(n, \alpha)^{77}$Ge reaction [4,39], the peak height of 0.264 MeV γ rays is smaller as compared to peak height of 0.66 MeV γ rays due to ^{80}As produced through the ^{80}Se$(n, p)^{80}$As reaction. In the 0.264 MeV photo peak the contribution of ^{77}Ge must be small due to irradiation time, which is much smaller as compared to the half life of ^{77}Ge radioisotope.

As observed in Figs. 3 and 4, the theoretical cross sections of ^{78}Se$(n, p)^{78}$As and ^{80}Se$(n, p)^{80}$As reactions estimated by EMPIRE-II code are found to increase initially with neutron energy, but starts decreasing with further increase in the

TABLE VIII. Cross sections for ^{80}Se$(n, p)^{80}$As reaction estimated over 13.73 MeV to 14.77 MeV neutron energies using different level density options of TALYS code and considering exciton model preeqmode 1.

Neutron energy (MeV)	Theoretical cross section (mb)		
	ldmodel 1	ldmodel 2	ldmodel 3
13.73	5.55	32.21	5.75
14.07	6.51	34.25	6.77
14.42	7.61	34.44	7.93
14.68	8.75	33.62	9.11
14.77	9.10	34.18	9.47

neutron energy above 16 MeV and 19 MeV respectively. This decrease in the cross section above 16 MeV neutron energy for the ^{78}Se$(n, p)^{78}$As reaction can be attributed to competing reaction channels [41] for ^{78}Se$(n, pn)^{77}$As and ^{78}Se$(n, 3n)^{76}$Se reactions having threshold energies $\sim$10.53 MeV and $\sim$18.15 MeV [10], respectively. Similarly, for the ^{80}Se$(n, p)^{80}$As reaction the decrease in the cross section with neutron energy can be attributed to the competing reaction channels [41] for ^{80}Se$(n, pn)^{79}$As and ^{80}Se$(n, 3n)^{78}$Se reactions having threshold energies $\sim$ 11.56 MeV and $\sim$ 17.09 MeV [10] respectively. As observed in Figs. 3 and 4, the estimated cross sections for ^{78}Se$(n, p)^{78}$As and ^{80}Se$(n, p)^{80}$As reactions by EMPIRE-II code deviates significantly from those of obtained by TALYS code around 15 MeV and 16 MeV neutron energy respectively. However, for the ^{78}Se$(n, p)^{78}$As reaction the cross sections reported by Hoang up to 16.6 MeV neutron energy are close to those estimated by EMPIRE-II code but deviates significantly from those estimated by TALYS code. The cross sections of ^{78}Se$(n, p)^{78}$As and ^{80}Se$(n, p)^{80}$As reactions estimated
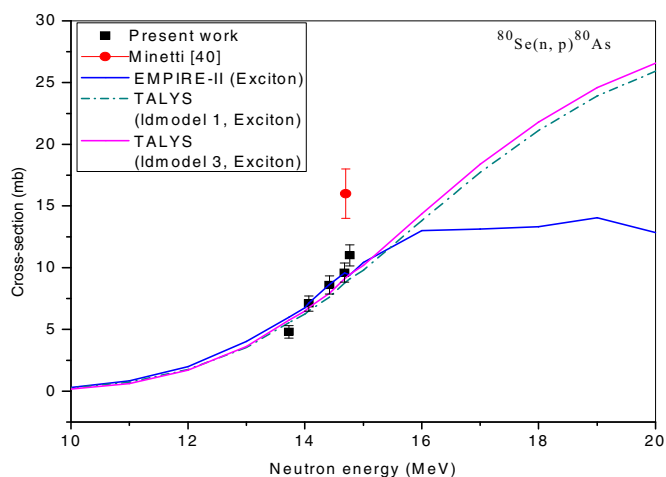

FIG. 4. (Color online) Cross sections for ^{80}Se$(n, p)^{80}$As reaction at different neutron energies (i) measured in the present work and (ii) estimated over 10 MeV to 20 MeV neutron energies using EMPIRE-II and TALYS codes in the present work. One literature cross section is given for comparison.

TABLE IX. Cross sections for ^{80}Se$(n, p)^{80}$As reaction (i) measured in the present work and (ii) theoretically estimated using EMPIRE-II and TALYS codes over 13.73 MeV to 14.77 MeV neutron energies using the best close options.

Neutron energy (MeV)	Theoretical cross section (mb)		Measured cross section (mb)
	EMPIRE-II (Exciton model, EMPIRE specific, Bechetti)	TALYS (Exciton model, ldmodel 3)	
13.73	5.97	5.75	4.8 ± 0.63
14.07	7.13	6.77	7.1 ± 0.95
14.42	8.64	7.93	8.6 ± 1.1
14.68	9.57	9.11	9.6 ± 1.4
14.77	9.41	9.47	11 ± 1.6

by TALYS code are found to increase continuously with neutron energy used in the present work. These results are not consistent because the cross sections of ^{78}Se$(n, p)^{78}$As and ^{80}Se$(n, p)^{80}$As reactions must decrease above the neutron energy at which other (n, pn), $(n, 3n)$, etc. nuclear reactions are induced through the other channels.

The thresholds for the formation of ^{78}As and ^{80}As through ^{80}Se$(n, 2np)^{78}$As and ^{82}Se$(n, 2np)^{80}$As reactions are above 20 MeV and therefore no interference was possible in the measured cross sections of ^{78}Se$(n, p)^{78}$As and ^{80}Se$(n, p)^{80}$As reactions, respectively. The ^{80}As has a short half life of 15.2 s and therefore the cross sections reported in the present work for the ^{80}Se$(n, p)^{80}$As reaction can be used for the estimation of selenium in a sample without risk of formation of long-life arsenic radioisotopes. The production of harmful isotopes of arsenic can be minimized by avoiding use of the selenium in the accelerator areas where high-energy neutrons are produced.

[1] IAEA Nuclear Data Services, http://www-nds.iaea.org/exfor/exfor.htm

[2] V. Avrigeanu, S. V. Chuvaev, R. Eichin, A. A. Filatenkov, R. A. Forrest, H. Freiesleben, M. Herman, A. J. Koning, and K. Seidel, Nucl. Phys. A **765**, 1 (2006).

[3] F. M. D. Attar, R. Mandal, S. D. Dhole, A. Saxena, Ashokkumar, S. Ganesan, S. Kailas, and V. N. Bhoraskar, Nucl. Phys. A **802**, 1 (2008).

[4] JAEA Nuclear Data Center, http://nucleardata.nuclear.lu.se/database/masses; http://wwwndc.jaea.go.jp/j33fig/jpeg/se078-f3.jpg

[5] M. Herman, *EMPIRE-II Statistical Model Code for Nuclear Reaction Calculations* (ver. 2.18 Mondovi) (IAEA, Vienna, Austria, 2002).

[6] A. J. Koning, S. Hilaire, and M. Duijvestijn, *TALYS-0.64*, A Nuclear Reaction Program, NRG - 1755 ZG Petten, The Netherlands, CEA, Service de Physiue et Techniques Nucleariques, B.P. 12, F-91680 Bruyeres-le-Chatel, France (2004).

[7] V. N. Bhoraskar, Indian J. pure Appl. Phys. **16**, 60A (1990).

[8] Reference neutron activation library, IAEA-TECDOC-1285, April (2002).

[9] C. M. Lederer, J. M. Hollander, and I. Perlman, *Table of Isotopes* (Berkeley, California, 1967).

[10] National Nuclear Data Center, http://www.nndc.bnl.gov

[11] J. K. Tuli, *Nuclear Wallet cards* (National Nuclear Data Center, Brookhaven, 2000).

[12] J. R. Taylor, *An Introduction to Error Analysis* (University Science Books, Mill Valley, 1982).

[13] K. Kawade, H. Sakane, Y. Kasugai, M. Shibata, T. Iida, A. Takahashi, and T. Fukahori, Nuclear Instruments and Methods in Physics Research A **496**, 183 (2003).

[14] http://www.physics.nist.gov/PhysRefData/XrayMassCoef/ElemTab/z34.html

[15] A. A. Filatenkov, S. V. Chuvaev, V. N. Aksenov, V. A. Yakovlev, A. V. Malyshenkov, S. K. Vasil'ev, M. Avrigeanu, V. Avrigeanu, D. L. Smith, Y. Ikeda, A. Wallner, W. Kutschera, A. Priller, P. Steier, H. Vonach, G. Mertens, and W. Rochow, Khlopin Radiev. Inst., Leningrad Reports No. 252 (1999).

[16] I. A. Reyhancan, Ann. Nucl. Energy **30**, 1001 (2003).

[17] E. Betak and P. Oblozinsky, "Code PEGAS", INDCCSLK-OOl, IAEA, Vienna (1993). DEGAS is 1996 improvement by E. Betak.

[18] H. Nishioka, J. J. M. Verbaarschot, H. A. Weidenmuller, and S. Yoshida, Ann. Phys. (N.Y.) **172**, 67 (1986).

[19] T. Tamura, T. Udagawa, and H. Lenske, Phys. Rev. C **26**, 379 (1982).

[20] A. V. Ignatyuk, G. N. Smirenkin, and A. S. Tishin, Sov. J. Nucl. Phys. **21**, 255 (1975).

[21] T. Ericson, Adv. Phys. **9**, 425 (1960).

[22] A. Gilbert and A. G. W. Cameron, Can. J. Phys. **43**, 1446 (1965).

[23] P. Demetriou and S. Goriely, Nucl. Phys. A **695**, 95 (2001).

[24] A. J. Koning and J. P. Delaroche, Nucl. Phys. A **713**, 231 (2003).

[25] F. D. Bechetti, Jr. and G. W. Greenless, Phys. Rev. **182**, 1190 (1969).

[26] A. S. Ilijinov, M. V. Mebel, N. Bianchi, E. De Sanctis, C. Guaraldo, V. Lucherini, V. Muccifora, E. Polli, A. R. Reolon, and P. Rossi, Nucl. Phys. A **543**, 517 (1992).

[27] A. R. Junghans, M. De Jong, H. G. Clerc, A. V. Ignatyuk, G. A. Kudyaev, and K. H. Schmidt, Nucl. Phys. A **629**, 635 (1998).

[28] S. Goriely, E. Tondeur, and J. M. Pearson, Atom. Data Nucl. Data Tables **77**, 311 (2001).

[29] A. J. Koning and M. C. Duijvestijn, Nucl. Phys. A **744**, 15 (2004).

[30] H. Gruppelaar, P. Nagel, and P. E. Hodgson, Riv. Nuovo Cimento **9**, 1 (1986).

[31] E. Gadioli and P. E. Hodgson, *Preequilibrium Nuclear Reactions* (Oxford University Press, Oxford, 1992).

[32] A. J. Koning and J. M. Akkermans, Ann. Phys. (NY) **208**, 216 (1991).

[33] C. Kalbach, Phys. Rev. C **37**, 2350 (1988).

[34] Guozhu He, Zhongjie Liu, Junhua Luo, and Xiangzhong Kong, Indian J. Pure Appl. Phys. **43**, 729 (2005).

[35] A. A. Filatenkov and S. V. Chuvaev, Khlopin Radiev. Inst., Leningrad Reports No. 258 (2001).

[36] I. Birn, S. M. Qaim, B. Strohmaier, and H. Freiesleben, Nucl. Sci. Eng. **116**, 125 (1994).

[37] A. Grallert, J. Csikai, Cs. M. Buczko, and I. Shaddad, IAEA Nucl. Data Section report to the I.N.D. C. No.286, 131 (1993).

[38] H. M. Hoang, U. Garuska, A. Marcinkowski, and B. Zwieglinski, Zeitschrift fuer Physik A, Hadrons and Nuclei **334**, 285 (1989).

[39] ENDF: Evaluated Nuclear Data File, https://www-nds.iaea.org

[40] B. Minetti and A. Pasquarelli, Nuclear Physics, Section A **100**, 186 (1967).

[41] J. M. Blatt and V. F. Weisskopf, *Theoretical Nuclear Physics* (Wiley, New York, 1966).